Published in final edited form as:
Free Radic Biol Med. 2009 August 15; 47(4): 410–418. doi:10.1016/j.freeradbiomed.2009.05.003.

Early onset senescence occurs when fibroblasts lack glutamate cysteine ligase modifier subunit

Ying Chen[a,b,*], **Elisabet Johansson**[a], **Yunxia Fan**[a], **Howard G. Shertzer**[a], **Vasilis Vasiliou**[b], **Daniel W. Nebert**[a], and **Timothy P. Dalton**[a]

[a] Department of Environmental Health and Center for Environmental Genetics (CEG), University of Cincinnati Medical Center, Cincinnati, OH 45267-0056, USA

[b] Department of Pharmaceutical Sciences, School of Pharmacy, University of Colorado Denver, Aurora, CO 80045, USA

Abstract

Cellular senescence is the irreversible entry of cells into growth arrest. Senescence of primary cells in culture has long been used as an in vitro model for aging. Glutamate cysteine ligase (GCL) controls the synthetic rate of the important cellular antioxidant glutathione (GSH). The catalytic subunit of GCL, GCLC, is catalytically active and essential for life. By contrast the modifier subunit of GCL, GCLM, is dispensable in mice. Although GCLM is recognized to increase the rate of GSH synthesis, its physiological role is unclear. Herein, we show that loss of *Gclm* leads to premature senescence of primary murine fibroblasts as characterized by: (a) diminished growth rate; (b) cell morphology consistent with senescence; (c) increases in senescence-associated β-galactosidase activity; and (d) cell cycle arrests at the G_1/S and G_2/M boundary. These changes were accompanied by increased intracellular ROS, accumulation of DNA damage, and induction of p53 and p21 proteins. We also found that *N*-acetylcysteine (**NAC**) increases intracellular GSH and prevents premature senescence in *Gclm*(−/−) cells. These results suggest that the control of GCLM, which in turn controls aspects of the cellular redox environment via GSH, is important in determining the replicative capacity of the cell.

Keywords

Glutathione; oxidative stress; aging; cellular senescence; p53

Introduction

Glutamate cysteine ligase (GCL) catalyzes the synthesis of γ-glutamylcysteine (γ-GC) from glutamate and cysteine and is the rate-limiting enzyme in the synthesis of the abundant synthetic antioxidant glutathione (GSH) [1]. GCL of prokaryotes and perhaps the yeast saccaromyces cervisiae is encoded by a single gene [2–4]. GCL from multi-cellular eukaryotes consists of a monomeric catalytic subunit (GCLC), which possesses the capacity to synthesize γ-GC, and a heterodimeric holoenzyme complex (hereafter referred to as GCL) comprised of

*Corresponding author: University of Colorado Denver, School of Pharmacy, C238-P15 RC2, 12700 E. 19th Avenue, Room 3450A, Aurora CO 80045, USA. Tel: +1 303 724 3521; Fax: +1 303 724 7266; ying.chen@ucdenver.edu.

GCLC and a polypeptide known as glutamate cysteine ligase modifier subunit (GCLM). GCLM alters the catalytic properties of GCL, lowering the Km for the substrates glutamate and ATP, increasing the velocity of γ-GC synthesis and increasing the Ki for feedback inhibition by GSH [5]. GCLM is classified as a member of the aldo-keto reductase family of enzymes but can not itself catalyze the synthesis of γ-GC [6]; thus far it is not attributed with independent enzymatic activity.

In mice targeted ablation of *Gclc* is embryonic lethal; *Gclc*(−/−) mice cannot synthesize GSH [7]. By contrast targeted ablation of *Gclm* does not cause overt phenotype in mice, although GSH levels are decreased [6]. *Gclm*(−/−) mice are more sensitive to acetaminophen toxicity and cells from these mice are more sensitive to treatments of hydrogen peroxide, heavy metal and other compounds [6,8–12]. Thus in the absence of acute challenge with a toxicant, the role of *Gclm* is unclear. It seems possible, however, that loss of *Gclm* results in a persistent if mild oxidant stress and that cellular processes or programs sensitive to such a stress might be altered.

Glutathione (**GSH**), the most abundant intracellular thiol, is present in millimolar concentrations. GSH has several important functions [13]: (a) detoxifies xenobiotics and their metabolites, and some endogenous metabolites non-enzymatically or enzymatically (via the GSH *S*-transferase family) to form GSH conjugates ;(b) is essential in maintaining the intracellular redox balance and the thiol moieties of proteins;(c) functions as a major antioxidant to protect against oxidative damage caused by reactive oxygen species (**ROS**); (d) serves as a signaling molecule by post-translational modification of proteins; and (e) plays a role in the regulation of nitric oxide homeostasis. Due to one or more of these functions, GSH appears to participate in decisions of cell fate—including proliferation, differentiation, and apoptosis [14].

It was originally proposed in 1980's that oxidative stress was a causal factor in differentiation and aging [15,16]. The free radical theory of aging asserts that organisms age consequent to accumulated oxidant damage to cellular macromolecules. Several lines of evidence support the "free radical theory" of aging [17–19]: (a) Overproduction of ROS, and/or depletion of GSH by endogenous and exogenous stimuli, have been suggested to be involved in the pathogenesis of many aging-related diseases—including coronary heart disease, neurodegenerative disorders, and cancer; (b) Genetic studies in the worm, fly and mouse suggest a link between longevity and resistance to oxidative stress; (c) In cell culture systems, entry into the irreversible growth-arrest stage (termed "cellular senescence") can be induced by oxidative stress-causing agents such as H_2O_2, UV light, hyperoxia, and several chemotherapeutic drugs. Cellular senescence of primary human and mouse cells in culture has been used as a model to identify aging-associated changes at the molecular level. Extensive studies in this field in recent years have uncovered several important players in this process, and cellular senescence is increasingly recognized as a potential tumor suppressive mechanism, in addition to its role in aging of the intact animal [20,21].

"Replicative senescence" is a process that occurs in most types of normal primary cells, following an extended period of proliferation in culture; the cells begin to undergo a dramatic change in morphology and cellular metabolism [22–24]. Telomeric shortening (or uncapping) is the primary cause of this process in human fibroblasts, whereas physiological stress accumulated in culture conditions is believed to be the activator of replicative senescence in mouse fibroblasts [25]. Regardless of the species origin of the cells, extrinsic stimuli—including oxidative stress, DNA-damaging agents, and oncogene overexpression—can speed up this state of senescence, so that it occurs within a period of several days; in this case, the process is termed "stress-induced senescence" **(SIS)** [26–29]. Numerous studies suggest that both types of senescence are activated when cells accumulate damage to some critical level [30,31].

In this study, we used *Gclm*(−/−) mouse fetal fibroblast (**MFF**) to study the role of *Gclm*, and by extension GSH, in cellular aging in culture. We demonstrate that *Gclm*(−/−) fibroblasts undergo premature senescence at dramatically earlier passage in culture, compared with that for wild-type *Gclm*(+/+) fibroblasts. Because of the senescence-like morphology and increased senescence-associated β-galactosidase (**SA-β-gal**) activity, we also explored other molecular events associated with this phenotype.

Materials and methods

Chemicals

H_2O_2 and *N*-acetylcysteine (**NAC**) were purchased from Sigma (Sigma Aldrich Co. St. Louis, MO).

Cell Culture

Gclm(−/−) mice were generated as described [6]; the *Gclm*(−) allele has been backcrossed into the C57BL/6J background for more than nine generations. *Gclm*(+/−) heterozygotes were mated for timed pregnancies, with the day of the vaginal plug considered as gestational day (**GD**) 0.5. *Gclm*(+/+) and *Gclm*(−/−) mouse fetal fibroblasts (MFFs) were prepared from GD14.5 fetuses. Briefly, GD14.5 fetuses were individually dissected of head and viscera. Fetal heads were digested with proteinase K and genomic DNA prepared using DNeasy Blood and Tissue Kit (QIAGEN). Individual fetuses were genotyped as previously described [6]. Fetal bodies were rinsed twice in PBS, then minced in 4x volume (0.9–1.1 ml) of 0.25% trypsin plus 2 mM EDTA and passed twice through a syringe fitted with a 22 gauge needle. This cellular suspension was then incubated at 37°C for 20 min; dispersed cells from each fetus were resuspended in standard culture medium [DMEM supplemented with 10% FBS, 100 units/ml penicillin and streptomycin (Gibco BRL, Grand Island, NY)], and plated in individual 60-mm tissue culture dishes to grow overnight. On the next day, dead cells and debris were removed, and the viable cells were re-fed with standard medium. Cells at this stage were considered "passage zero" (**P0**). When these cells reached 90% confluency, $2 \times 10^4/cm^2$ cells were sub-cultured and considered as passage 1 (**P1**) and population-doubling number zero (**PD0**). Starting at this point, the cells were cultured in standard medium containing 0 or 5 mM NAC (added fresh daily, as indicated). When cells reached 90–95% confluency, cells were passaged at $2 \times 10^4/cm^2$ and considered as the next passage (P_{n+1}). At each passage, MFFs were harvested and subjected to measurements, as described below. At all times, MFF cells of the indicated genotypes were grown under standard culture conditions (37°C, 5% CO_2, 95% air), and FBS of the same lot number was always used for each independent set of experiments.

Cell growth rate assay and cell morphology

At each passage, viable MFFs were counted, using trypan-blue exclusion (Sigma). Population-doubling numbers were calculated as $PD = \log_2(N_f/N_0)$, where N_f is the final number of cells and N_0 is the number of cells that were initially seeded. Population-doubling time was calculated as PD time (in hours) = days in culture × 24/PD number. Cell morphology was examined by light microscopy, and representative images at indicated passages were obtained, using a Nikon Eclipse TE-300 microscope.

SA-β-gal staining

MFF cells were seeded at 2×10^5/well in 6-well plates, and SA-β-gal staining was performed as described [32]. The positive (blue-stained) cells were counted per 200 cells at 400x magnification, and the SA-β-gal activity was reported as the percentage of SA-β-gal positive cells.

Cellular GSH and H_2O_2 cytotoxicity

GSH levels in whole cell extracts were determined spectrophotofluorometrically using *o*-phthalaldehyde [33]. Results are reported as mM concentrations, based on the estimate of 1 mg protein ≈ 5 μl cell volume [34]. For cytotoxicity assays, H_2O_2 (100x) was added directly into the medium, and cell viability was determined by the 3-(4,5-dimethylthiazol-2-yl)-2,5-diphenyltetrazolium bromide (**MTT**) assay (Promega, Madison, WI) after 8 h. We have previously shown that MTT reduction indicates cell viability in MFF cultures treated as herein [6]. Results were reported as the comparative percentage of untreated control cells for each genotype.

Measurement of DNA strand breaks

Single- and double-stranded DNA strand breaks were determined, at the indicated passage numbers, using the alkaline comet assay, as described [35]. The extent of DNA damage was expressed by the total comet score, calculated as following: scores ranged from zero to 4, based on length of the comet tail with 0 = no tail, 1 = tail length less than nuclear diameter (**<1ND**), 2 = tail length <2ND, 3 = tail length >2ND, and 4 = DNA content becoming entirely the tail; total score = (percentage of cells in class 0) × 0 + (percentage of cells in class 1) × 1 + (percentage of cells in class 2) × 2 + (percentage of cells in class 3) × 3 + (percentage of cells in class 4) × 4. *Gclm*(+/+) cells, treated with 100 μM H_2O_2 for 2 h, were used as the positive control. Results are expressed as the total score of 200 cells.

Flow cytometric analysis for cell cycle progression, apoptosis and ROS

Fluorescence-activated cell sorter (**FACS**) cytometry was performed on a FACS-Calibur cytometer (Becton Dickinson), and results were analyzed using the software provided by the manufacturer. For cell-cycle progression analysis, MFFs were seeded at 2×10^4 cells/cm^2 and grown in standard culture medium for 48 h. MFFs were then collected for cell-cycle distribution analysis by flow cytometry. DNA was stained by propidium iodide (**PI**), and the fraction of cells in the G_0-G_1, S, and G_2/M phases was determined from the fraction of cells having 2N, 2N-4N, and 4N DNA content, respectively. The fraction of apoptotic cells was determined by counting cells in the sub-G_1 peak.

For measurements of ROS, MFFs were seeded at 2×10^5/well in 6-well plates and grown in standard culture medium for 24 h. Cells were then washed twice with pre-warmed serum-free DMEM, followed by incubation in serum-free DMEM containing 5 μM 5-(and-6-) chloromethyl-2′7′-dichlorodihydrofluorescein diacetate acetyl ester (CM-H_2DCFDA) (Invitrogen) for 30 min at 37°C; cells were then collected and immediately analyzed by flow cytometry. The fluorescence intensity of DCF, the oxidation product of CM-H_2DCFDA, was determined using excitation and emission wavelengths of 495 and 525 nm, respectively. Mean log fluorescence intensity values were obtained by the CELLQUEST software (BD Bioscience). The value for *Gclm*(+/+) cells at **P1** was set as base line, and the ratio to this value is expressed as the relative ROS level.

Reverse transcription and real-time quantitative PCR

MFF cells were seeded at 1.2×10^6 in 60-mm culture dishes, and total cellular RNA was isolated using Tri Reagent (Molecular Research Center, Inc.). First-strand cDNA was synthesized from total RNA (1 μg) with SuperScript®III First-Strand cDNA Synthesis kit (Invitrogen). Reaction mixtures of 20 μl—containing 125 nM gene-specific primer sets, 1 μl of cDNA template, and 10 μl of iQ™SYBR Green Supermix (Bio-Rad)—were used for real-time quantitative PCR (**Q-PCR**) in a DNA Engine Opticon-2 Real-Time PCR Detection System (MJ Research). Results were analyzed using the software provided by the manufacturer. Primers used in Q-PCR included: 5′-TGGAAGACTCCAGTGGGAAC-3′ (forward) and 5′-

TCTTCTGTACGGCGGTCTCT-3′ (reverse) for p53, encoded by the *Trp53* gene; 5′-GAACAGGGATGGCAGTTAGG-3′ (forward) and 5′-AGTATGGGGTGGGGGAAAAG-3′ (reverse) for p21, encoded by the *Cdkn1a* gene. Relative mRNA levels for each gene are reported relative to the control level in *Gclm*(+/+) cells at passage one (**P1**), after normalization with β-actin.

Western immunoblot analysis for p53 and p21

MFFs were seeded at 2×10^6 cells in each 10 cm^2 dish and nuclear extracts were prepared as previously described [36] and separated by SDS-PAGE. Western immunoblot analysis was conducted using rabbit polyclonal antibody (1:500, Santa Cruz) to detect p53 protein, and using mouse monoclonal antibody (1:20, Oncogene) to detect p21 protein. β-actin was used as the loading control.

Statistical analysis

Statistics were performed using SigmaStat Statistical Analysis software (SPSS Inc., Chicago, IL). Group means were compared by one-way ANOVA, followed by the Tukey post-hoc test for pairwise comparison. Results are reported as the means ± S.E. of 6–8 or 3–4 individual cell cultures for each group for growth rate assays or all other measurements, respectively. All p values <0.05 were regarded as statistically significant.

Results

Loss of Gclm induces premature senescence in primary fibroblasts

Cellular senescence is responsible for the finite replication of most somatic cells in culture, and this process can be induced by extrinsic stimuli, including oxidants stress, in pre-senescent cells in the case of SIS. Loss of *Gclm* in mice results in 60–90% depletion of tissue GSH levels, albeit without causing observable abnormalities in the intact animal [6]. To investigate the role of GCLM in cellular senescence, *Gclm*(−/−) MFFs were used to study the cellular growth in culture. MFFs were prepared from GD14.5 fetus from *Gclm*(+/−) intercrossing, and fetus of three possible genotypes showed no difference in general appearance and body weight (data not shown).

Gclm(+/+) and *Gclm*(−/−) cells were seeded at equal density (~25% confluency) at each passage, and cellular growth was evaluated. Cells of both genotypes at early passage (P1–P4) showed similar growth rates (Fig. 1); however, *Gclm*(−/−) cells revealed premature growth inhibition starting at P5, which occurred at the maximal population-doubling (MPD) of 10 ± 0.2 (compared with MPD of 16 ± 0.5 for *Gclm*(+/+) cells at P10). Due to the number of parameters being measured and the dramatic decrease in growth rate in *Gclm*(−/−) cell cultures, we could not study *Gclm*(−/−) cells beyond P8.

Starting at P5, many *Gclm*(−/−) cells became enlarged, flattened and more transparent, with a decreased nucleus-to-cytoplasm ratio (Fig. 2A); this is typical of senescent cells. Senescence-associated β-gal (**SA-β-gal**) activity is a well-established biochemical marker for the senescent phenotype [32]. Cells positively stained for SA-β-gal were determined to be ~32% and ~50% of *Gclm*(−/−) cells at P5 and P7, respectively (Figs. 2B & 2C); in contrast, *Gclm*(−/−) cells at passages earlier than P5, and *Gclm*(+/+) cells at all passages, revealed positive staining for SA-β-gal at control levels (~7%).

Growth arrest at the G_1/S and G_2/M boundary in senescent Gclm(−/−) cells

Based on the cell growth rate assay (Fig. 1), compared with *Gclm*(+/+) wild-type cells, *Gclm*(−/−) cells showed a prolonged cell-cycle starting at P5, as indicated by an increased PD time (Fig. 3); at this passage, *Gclm*(−/−) cells displayed senescent phenotype (Fig. 2). To study the

nature of growth inhibition observed in senescent *Gclm*(−/−) MFFs, we analyzed cell population distribution in cell-cycle progression by flow cytometry using propidium iodide statining. Compared with *Gclm*(+/+) cells, the S phase populations in *Gclm*(−/−) cell cultures were greatly decreased by P5 and P7, accompanied by increased cell populations in G_0-G_1 and G_2-M phases (Fig. 3). The flow-cytometry data suggest that growth arrest in senescent *Gclm*(−/−) cells occurs at the G_1/S and G_2/M boundaries. Such growth arrest has been reported previously as a feature of senescent cells [37]. It is worth noting that, during our flow-cytometry analysis, the percent of apoptotic cells in the *Gclm*(−/−) versus *Gclm*(+/+) cells was not different, at any of the passages (1.1 ± 0.1% and 1.2 ± 0.09%, respectively, for all passages combined).

Increased intracellular ROS and DNA damage in Gclm(−/−) cells

Loss of GCLM renders *Gclm*(−/−) mice and cells highly susceptible to exogenous oxidative insults, due to deficiency in GSH *de novo* biosynthesis [6,8–12]. We postulated that *Gclm*(−/−) MFFs should sensitize to endogenous oxidative stress, which could potentially be the inducer of premature senescence. To evaluate intracellular redox status along cell propagation in culture, we first measured the intracellular GSH levels at each alternate passage (Fig. 4A). From P1 to P9, there was a downward trend in GSH levels in the wild-type cells; nevertheless, the GSH in *Gclm*(−/−) cells, relative to that in *Gclm*(+/+) cells, decreased to ~25% by P5 and to ~16% at P7. The enhanced sensitivity to H_2O_2-induced cell death (100 μM for 8 h) was ~10-fold greater in *Gclm*(−/−) cells than that in *Gclm*(+/+) cells and independent of passage numbers (Fig. 4B). For both *Gclm*(−/−) and *Gclm*(+/+) cells (Fig. 5A), the level of intracellular ROS rose, as a function of increasing passage number; however, ROS levels in *Gclm*(−/−) cells began >2-fold higher and remained higher than that in *Gclm*(+/+) cells at all passages. Genomic DNA damage was determined by the alkaline comet assay, which detects both single-stranded and double-stranded DNA breaks. DNA damage (Fig. 5B) was significantly higher in *Gclm*(−/−) cells, as indicated by higher total comet scores, than in *Gclm*(+/+) cells through P7, and increases in DNA damage intensified in senescent *Gclm*(−/−) cells (at P5~P7).

Induction of p53 and p21 in senescent Gclm(−/−) cells

Activation of p53 plays a key role in the process of cellular senescence in murine fibroblasts; numerous cellular stresses, including oxidative stress, can serve as upstream stimuli to activate p53 leading to premature senescence [38,39]. To determine if p53 activation and its function are associated with the premature senescent phenotype observed in *Gclm*(−/−) cells, we examined the mRNA and protein levels of p53 and its downstream target p21. Q-PCR analysis (Fig. 6A) showed that the mRNA level of p53 was not different between *Gclm*(+/+) and *Gclm*(−/−) cells, and did not change as a function of increasing passages for either genotype; on the contrary, p21 mRNA was up-regulated 6.5-fold in senescent *Gclm*(−/−) cells (P5 & P7). For the purposes of comparison, the mRNA level of each gene in *Gclm*(+/+) cells at P1 was set as the control, and relative mRNA levels were reported as fold of control. On the other hand, western immunoblot analysis (Fig. 6B) using nuclear extracts revealed a dramatic increase of both p53 and p21 proteins in senescent *Gclm*(−/−) cells (at P5 ~ P7). It should be noted that, compared with *Gclm*(+/+) cells at similar passages, modest induction of p21 protein was also detected in pre-senescent *Gclm*(−/−) cells.

Rescue of premature senescence in Gclm(−/−) cells by NAC

All the previous convergent experiments strongly suggest that *Gclm*(−/−) MFFs undergo premature senescence due to enhanced oxidative stress, which is most likely brought on by decreased intracellular GSH levels. To test further this cause-and-effect relationship, we supplemented the standard culture medium with *N*-acetylcysteine. In both *in vivo* and *in vitro* studies, NAC has commonly been used to increase GSH levels by supplying the rate-

limiting substrate cysteine for GSH biosynthesis [40]. In addition NAC itself is an antioxidant [41] and may act to spare GSH. As shown in Fig. 7, NAC supplementation, at 5 mM in the culture medium starting at P1, increased the intracellular GSH levels in both *Gclm*(+/+) and *Gclm*(−/−) cells (comparing Figs. 7A and 4A); the levels in *Gclm*(−/−) cells were somewhat lower, but not statistically significantly lower, than that in *Gclm*(+/+) cells. In agreement with the increases in intracellular GSH, the levels of intracellular ROS were lowered by NAC treatment; although the levels in treated *Gclm*(−/−) cells remained higher than that in *Gclm*(+/+) cells, they were comparable to the levels seen in pre-senescent *Gclm*(−/−) cells (Fig. 7B). Similarly, the extend of DNA damage as measured by total comet score was diminished to the control levels in *Gclm*(−/−) cells by NAC treatment (comparing Figs. 7C and 5B). Accompanying all these changes, the premature senescent phenotype seen in non-NAC-treated *Gclm*(−/−) cells was completely prevented by NAC. NAC-treated *Gclm*(−/−) cells displayed the same proliferative profile as for NAC-treated *Gclm*(+/+) cells (Fig. 7D). Also, normal morphology of pre-senescent cells and only negligible positive staining for SA-β-gal activity were seen at P9 (Fig. 7E).

Discussion

GCL is necessary for the synthesis of GSH, as it is the enzyme that produces the unique γ-glutamyl covalent bond found in GSH. Indeed, GCL is the rate-limiting and committing step in the synthesis of GSH. The final step catalyzed by GSH synthetase apparently proceeds efficiently in all cell types, leaving the concentration of γ-GC extremely low while GSH reaches mM concentrations [1]. GCLC is necessary for the production of γ-GC and *Gclc* is essential for embryonic development attesting to essential functions of GSH [7]. Gel filtration analysis of hepatic cytosolic fractions demonstrated that GCLM is the sole dimerization partner for GCLC [6]. In the presence of GCLM, the catalytic characteristics of the GCL holoenzyme is dramatically altered allowing the efficient production of γ-GC and consequently GSH [5]. The important role of GCLM in maintaining tissue GSH levels has been clearly demonstrated in *Gclm*(−/−) mice, which possess between 60 and 90% less GSH depending on the tissue or cell-type assayed [6]. Surprisingly, these mice display no overt phenotype unless challenged with a toxicant [6,12]. Did *Gclm* evolve to serve a protective role following calamitous environmental insults or does it serve more subtle endogenous functions?

In this study, we show that murine primary fibroblasts which lack *Gclm*, undergo premature senescence in culture—as revealed by a decreased growth rate, surviving fewer passages before reaching final growth arrest, and early senescence-associated morphological and biochemical changes. This phenotype is accompanied by elevated levels of intracellular ROS and accumulation of DNA damage. These results suggest that further experiments in *Gclm*(−/−) mice should be conducted to examine pathophysiological abnormalities with age. Perhaps human epidemiological studies may offer clues as to organ systems most affected by loss of GCLM function. It has been demonstrated that risk of myocardial infarction is increased by functional SNPs in both the *GCLC* and *GCLM* genes [42,43]. In addition, SNPs in *GCLM* have been associated with the development of schizophrenia [44].

The level of GCLM is controlled at the level of transcription and perhaps also translation [45]. Furthermore, post-translational modifications to GCLC may occur in some cell types that block its interaction with GCLM [5]. Thus, there are multiple ways the interaction of GCLM with GCLC is regulated. It is therefore reasonable to speculate that genetic polymorphisms in regulatory (e.g. transcription factors or protein kinases) might also be associated with the interaction of GCLC and GCLM and consequently GSH levels.

GCLM possesses the signature sequence necessary to be classified as an aldo/keto reductase, although no catalytic activity has been reported for isolated GCLM. Upon discovering that loss

of *Gclm* led to premature senescence, we were interested in determining if this phenotype was associated with GCLM's role in GSH homeostasis or perhaps a different enzymatic role. Our results suggest that premature senescence is the consequence of GSH depletion in *Gclm*(−/−) cells, because these cells are entirely rescued by NAC supplementation. NAC treatment increases intracellular GSH in *Gclm*(−/−) cells toward control levels, but it would not be expected to compensate for direct enzymatic functions of GCLM. Furthermore, our results support conclusions from other studies that, when increased accumulation of DNA damage reaches a critical level, senescence in cell cultures is triggered [46–48]. In our model system, *Gclm* null MFFs, the excessive accumulation of DNA damage is a consequence of chronic endogenous oxidative stress resulted from GSH deficiency.

GSH, together with its oxidized form GSSG, represent the major cellular redox buffer. Changes in GSH/GSSG ratio may modulate the functions of proteins, that are sensitive to cellular redox environment, through cysteine residues in their active sites; a number of these proteins are critical players involved in signal transduction, cell proliferation, differentiation and death, including stress kinases, transcriptional factors and caspases [49,50]. In addition, mitochondrial GSH is essential in maintaining mitochondrial structural and functional integrity; disruption of this integrity leads to overproduction of ROS and may directly mediate cell death [51]. It has been shown in cultured-cell models that an increase in cellular GSH promotes cell proliferation as seen in some cancer cell lines [52]; acute deficiency in GSH, on the other hand, results in transient growth inhibition or induction of apoptosis [53]. Herein, we provide new evidence supporting the notion that GSH homeostasis is a critical determinant in the process of cellular senescence [54,55].

Studies from laboratories of other investigators have shown that, during the aging process, cellular GSH/GSSG ratio declines progressively, due to a decrease in GSH and/or an increase in GSSG, in human fibroblasts [56,57], mouse [58] and insects [59,60]. It is also suggested that *de novo* GSH synthetic capacity is compromised during aging, for that GCL in aged organisms has much lower affinities for its substrates glutamate and cysteine than in young ones of the same species [61,62]. The direct role of disrupted cellular GSH homeostasis in contributing to aging process, however, is evidenced in studies showing shortened proliferative span of human fibroblasts *in vitro* by GCLC inhibitor *L*-buthionine-sulfoximine (BSO) [63] and an expanded life span in *Drosophila* overexpressing GCLC or GCLM [64], and as well as in present study demonstrating that premature senescence occurs in fibroblast cultures lacking GCLM. More importantly, our study along with others indicate that loss of GCLM or overexpression of GCL is sufficient to accelerate cellular senescence or decelerate aging, respectively, by modifying cellular GSH levels.

In *Gclm*(−/−) MFFs, premature senescence occurs when cellular GSH is depleted by ~75%. In another cell culture system, with more severe GSH deficiency due to the absence of GCLC protein, quite different phenomena have been observed. *Gclc*(−/−) cells derived from blastocysts inner mass grow indefinitely in culture when maintained in either 2.5 mM GSH or 2–5 mM NAC [65]; these cells have <2% of wild-type intracellular GSH levels and, withdrawal of GSH from the medium triggers apoptosis [66]. Such phenotypic differences may be due to the ability of stem cells to bypass cellular senescence, or alternatively, suggest a cell-specific role of GSH in the process of cellular senescence. It is worth noting that NAC supplementation equally slows down the growth rate of both *Gclm*(+/+) and *Gclm*(−/−) cells (comparing Figs. 1 and 7D); this phenomenon has been reported previously in the study of *Gclc*(−/−) blastocyts [65]. The growth inhibition by NAC supplementation in our cell system is due to a cell cycle prolongation exclusively in G_0-G_1 phase, according to flow-cytometry analysis (data not shown). These NAC-treated cells maintain proper pre-senescent cell morphology, having a higher nucleus-to-cytoplasm ratio as late as P9. The physiological significance of this observation is not known.

Oxidant stress is a common signal which has been shown to promote cellular growth, senescence and death [38,53]. The decision as to which of the three endpoints is chosen by the cell likely depends on the cell type, the level and duration of such intracellular stress, all of which may dictate which downstream signaling pathway(s) is(are) activated and to what degree. Indeed, it has been proposed that replicative senescence may be associated with a constantly modest stress on the cell population, whereas a large amount of stress tends to induce a more dramatic cellular response manifesting apoptotic or necrotic death [67]. In the current study, we show that loss of *Gclm* in fibroblasts favors senescence as opposed to other cell fates.

The tumor suppressor p53 is believed to be a key regulatory protein involved in all three cellular events [38,68,69]. Our study showed that activation of p53→p21 pathway is involved in premature senescence seen in *Gclm*(−/−) cells. Induction of p53 protein is due to increased protein stability, as the mRNA levels of p53 remain unchanged; this is consistent with the notion that p53 activity is primarily controlled by post-translational modification [70]. On the other hand, p21 protein is upregulated at the transcriptional level, at least in part by p53 activation. The signaling pathways involved in p53 activation and the precise mechanisms underlying this premature senescence phenotype require further investigation. Our preliminary data showed that the mRNA level of p19 remained unchanged in senescent *Gclm*(−/−) cells, indicating that p19 is not likely the upstream activator of p53 (data not shown); enhanced mRNA level of p16 was also observed in *Gclm*(−/−) cells, albeit independent of the premature senescence phenotype (data not shown).

In summary, this study demonstrates that loss of GCLM protein results in premature senescence; such phenotype can be prevented by GSH increasing compound NAC. These results suggest that the control of GCLM, which in turn controls aspects of the cellular redox environment via GSH, is important in determining the replicative capacity of the cell. Future studies aiming at the identification of key players in signaling an accelerated cellular aging process in *Gclm*(−/−) MFF model system is of great potential to enhance our understanding of the oxidative mechanisms underlying cellular aging. In the same line, further analysis on parameters of cellular aging in intact *Gclm*(−/−) mouse with age holds promise for providing new information regarding the role of GSH homeostasis in aging *in vivo*.

Acknowledgments

We thank our colleagues for discussions and a careful reading of this manuscript. Much of this work was presented at the 45th Annual Meeting of the Society of Toxicology, San Diego, CA (March, 2006). This work was funded, in part, by NIH grants R01 ES012463 (T.P.D. and H.G.S.), P30 ES06096 (T.P.D., D.W.N., H.G.S) and R01 EY017963 (V.K.V).

Abbreviations

GSH	glutathione
GCLC	glutamate-cysteine ligase catalytic subunit
GLCM	glutamate-cysteine ligase modifier subunit
ROS	reactive oxygen species
SIS	stress induced senescence
GD	gestational day
MFFs	mouse fetal fibroblasts
PD	population doubling

NAC	*N*-acetylcysteine
γ-GC	γ-glutamylcysteine
SA-β-gal	senescence-associated β-galactosidase
Q-PCR	real-time quantitative PCR

References

1. Meister A, Anderson ME. Glutathione. Annu Rev Biochem 1983;52:711–760. [PubMed: 6137189]
2. Lueder DV, Phillips MA. Characterization of Trypanosoma brucei gamma-glutamylcysteine synthetase, an essential enzyme in the biosynthesis of trypanothione (diglutathionylspermidine). J Biol Chem 1996;271:17485–17490. [PubMed: 8663359]
3. Kelly BS, Antholine WE, Griffith OW. Escherichia coli gamma-glutamylcysteine synthetase. Two active site metal ions affect substrate and inhibitor binding. J Biol Chem 2002;277:50–58. [PubMed: 11675389]
4. Ohtake Y, Yabuuchi S. Molecular cloning of the gamma-glutamylcysteine synthetase gene of Saccharomyces cerevisiae. Yeast 1991;7:953–961. [PubMed: 1687097]
5. Chen Y, Shertzer HG, Schneider SN, Nebert DW, Dalton TP. Glutamate cysteine ligase catalysis: dependence on ATP and modifier subunit for regulation of tissue glutathione levels. J Biol Chem 2005;280:33766–33774. [PubMed: 16081425]
6. Yang Y, Dieter MZ, Chen Y, Shertzer HG, Nebert DW, Dalton TP. Initial characterization of the glutamate-cysteine ligase modifier subunit Gclm(−/−) knockout mouse. Novel model system for a severely compromised oxidative stress response. J Biol Chem 2002;277:49446–49452. [PubMed: 12384496]
7. Dalton TP, Dieter MZ, Yang Y, Shertzer HG, Nebert DW. Knockout of the mouse glutamate cysteine ligase catalytic subunit (Gclc) gene: embryonic lethal when homozygous, and proposed model for moderate glutathione deficiency when heterozygous. Biochem Biophys Res Commun 2000;279:324–329. [PubMed: 11118286]
8. Giordano G, White CC, Mohar I, Kavanagh TJ, Costa LG. Glutathione levels modulate domoic acid induced apoptosis in mouse cerebellar granule cells. Toxicol Sci 2007;100:433–444. [PubMed: 17804861]
9. Giordano G, Kavanagh TJ, Costa LG. Neurotoxicity of a polybrominated diphenyl ether mixture (DE-71) in mouse neurons and astrocytes is modulated by intracellular glutathione levels. Toxicol Appl Pharmacol 2008;232:161–168. [PubMed: 18656495]
10. Lavoie S, Chen Y, Dalton TP, Gysin R, Cuenod M, Steullet P, Do KQ. Curcumin, quercetin and tBHQ modulate glutathione levels in astrocytes and neurons : Importance of the glutamate cysteine ligase modifier subunit. J Neurochem. 2009
11. Kann S, Estes C, Reichard JF, Huang MY, Sartor MA, Schwemberger S, Chen Y, Dalton TP, Shertzer HG, Xia Y, Puga A. Butylhydroquinone protects cells genetically deficient in glutathione biosynthesis from arsenite-induced apoptosis without significantly changing their prooxidant status. Toxicol Sci 2005;87:365–384. [PubMed: 16014739]
12. McConnachie LA, Mohar I, Hudson FN, Ware CB, Ladiges WC, Fernandez C, Chatterton-Kirchmeier S, White CC, Pierce RH, Kavanagh TJ. Glutamate cysteine ligase modifier subunit deficiency and gender as determinants of acetaminophen-induced hepatotoxicity in mice. Toxicol Sci 2007;99:628–636. [PubMed: 17584759]
13. Dalton TP, Chen Y, Schneider SN, Nebert DW, Shertzer HG. Genetically altered mice to evaluate glutathione homeostasis in health and disease. Free Radic Biol Med 2004;37:1511–1526. [PubMed: 15477003]
14. Sies H. Glutathione and its role in cellular functions. Free Radic Biol Med 1999;27:916–921. [PubMed: 10569624]
15. Sohal RS, Allen RG. Relationship between metabolic rate, free radicals, differentiation and aging: a unified theory. Basic Life Sci 1985;35:75–104. [PubMed: 4062824]

16. Sohal RS, Allen RG. Oxidative stress as a causal factor in differentiation and aging: a unifying hypothesis. Exp Gerontol 1990;25:499–522. [PubMed: 2097168]
17. Allen R. Oxidative stress and superoxide dismutase in development, aging and gene regulation. Age 1998;21:47–76.
18. Sohal RS, Mockett RJ, Orr WC. Mechanisms of aging: an appraisal of the oxidative stress hypothesis. Free Radic Biol Med 2002;33:575–586. [PubMed: 12208343]
19. Finkel T, Holbrook NJ. Oxidants, oxidative stress and the biology of ageing. Nature 2000;408:239–247. [PubMed: 11089981]
20. Collado M, Serrano M. The senescent side of tumor suppression. Cell Cycle 2005;4:1722–1724. [PubMed: 16294043]
21. Schmitt CA. Cellular senescence and cancer treatment. Biochim Biophys Acta. 2006
22. Campisi J. Cancer, aging and cellular senescence. In Vivo 2000;14:183–188. [PubMed: 10757076]
23. Narita M, Nunez S, Heard E, Narita M, Lin AW, Hearn SA, Spector DL, Hannon GJ, Lowe SW. Rb-mediated heterochromatin formation and silencing of E2F target genes during cellular senescence. Cell 2003;113:703–716. [PubMed: 12809602]
24. Sitte N, Merker K, Von Zglinicki T, Grune T, Davies KJ. Protein oxidation and degradation during cellular senescence of human BJ fibroblasts: part I--effects of proliferative senescence. FASEB J 2000;14:2495–2502. [PubMed: 11099467]
25. Itahana K, Campisi J, Dimri GP. Mechanisms of cellular senescence in human and mouse cells. Biogerontology 2004;5:1–10. [PubMed: 15138376]
26. Debacq-Chainiaux F, Borlon C, Pascal T, Royer V, Eliaers F, Ninane N, Carrard G, Friguet B, de Longueville F, Boffe S, Remacle J, Toussaint O. Repeated exposure of human skin fibroblasts to UVB at subcytotoxic level triggers premature senescence through the TGF-beta1 signaling pathway. J Cell Sci 2005;118:743–758. [PubMed: 15671065]
27. Lee S, Dorken B, Schmitt CA. Extracorporeal photopheresis in graft-versus-host disease: ultraviolet radiation mediates T cell senescence in vivo. Transplantation 2004;78:484–485. [PubMed: 15316381]
28. Marcotte R, Chen JM, Huard S, Wang E. c-Myc creates an activation loop by transcriptionally repressing its own functional inhibitor, hMad4, in young fibroblasts, a loop lost in replicatively senescent fibroblasts. J Cell Biochem 2005;96:1071–1085. [PubMed: 16167342]
29. Zdanov S, Remacle J, Toussaint O. Establishment of H2O2-induced premature senescence in human fibroblasts concomitant with increased cellular production of H2O2. Ann N Y Acad Sci 2006;1067:210–216. [PubMed: 16803987]
30. Ben Porath I, Weinberg RA. When cells get stressed: an integrative view of cellular senescence. J Clin Invest 2004;113:8–13. [PubMed: 14702100]
31. MacLaren A, Black EJ, Clark W, Gillespie DA. c-Jun-deficient cells undergo premature senescence as a result of spontaneous DNA damage accumulation. Mol Cell Biol 2004;24:9006–9018. [PubMed: 15456874]
32. Dimri GP, Lee X, Basile G, Acosta M, Scott G, Roskelley C, Medrano EE, Linskens M, Rubelj I, Pereira-Smith O. A biomarker that identifies senescent human cells in culture and in aging skin in vivo. Proc Natl Acad Sci U S A 1995;92:9363–9367. [PubMed: 7568133]
33. Senft AP, Dalton TP, Shertzer HG. Determining glutathione and glutathione disulfide using the fluorescence probe o-phthalaldehyde. Anal Biochem 2000;280:80–86. [PubMed: 10805524]
34. Watson WH, Jones DP. Oxidation of nuclear thioredoxin during oxidative stress. FEBS Lett 2003;543:144–147. [PubMed: 12753922]
35. Wang H, Yadav JS. DNA damage, redox changes, and associated stress-inducible signaling events underlying the apoptosis and cytotoxicity in murine alveolar macrophage cell line MH-S by methanol-extracted Stachybotrys chartarum toxins. Toxicol Appl Pharmacol 2006;214:297–308. [PubMed: 16476459]
36. Kann S, Huang MY, Estes C, Reichard JF, Sartor MA, Xia Y, Puga A. Arsenite-induced aryl hydrocarbon receptor nuclear translocation results in additive induction of phase I genes and synergistic induction of phase II genes. Mol Pharmacol 2005;68:336–346. [PubMed: 15894712]
37. Blagosklonny MV. Cell senescence: hypertrophic arrest beyond the restriction point. J Cell Physiol 2006;209:592–597. [PubMed: 17001692]

38. Ben Porath I, Weinberg RA. The signals and pathways activating cellular senescence. Int J Biochem Cell Biol 2005;37:961–976. [PubMed: 15743671]
39. Itahana K, Dimri G, Campisi J. Regulation of cellular senescence by p53. Eur J Biochem 2001;268:2784–2791. [PubMed: 11358493]
40. Sjodin K, Nilsson E, Hallberg A, Tunek A. Metabolism of N-acetyl-L-cysteine. Some structural requirements for the deacetylation and consequences for the oral bioavailability. Biochem Pharmacol 1989;38:3981–3985. [PubMed: 2597179]
41. Moldeus P, Cotgreave IA. N-acetylcysteine. Methods Enzymol 1994;234:482–492. [PubMed: 7808322]
42. Koide S, Kugiyama K, Sugiyama S, Nakamura S, Fukushima H, Honda O, Yoshimura M, Ogawa H. Association of polymorphism in glutamate-cysteine ligase catalytic subunit gene with coronary vasomotor dysfunction and myocardial infarction. J Am Coll Cardiol 2003;41:539–545. [PubMed: 12598062]
43. Nakamura S, Kugiyama K, Sugiyama S, Miyamoto S, Koide S, Fukushima H, Honda O, Yoshimura M, Ogawa H. Polymorphism in the 5′-flanking region of human glutamate-cysteine ligase modifier subunit gene is associated with myocardial infarction. Circulation 2002;105:2968–2973. [PubMed: 12081989]
44. Tosic M, Ott J, Barral S, Bovet P, Deppen P, Gheorghita F, Matthey ML, Parnas J, Preisig M, Saraga M, Solida A, Timm S, Wang AG, Werge T, Cuenod M, Do KQ. Schizophrenia and oxidative stress: glutamate cysteine ligase modifier as a susceptibility gene. Am J Hum Genet 2006;79:586–592. [PubMed: 16909399]
45. Wild AC, Mulcahy RT. Regulation of gamma-glutamylcysteine synthetase subunit gene expression: insights into transcriptional control of antioxidant defenses. Free Radic Res 2000;32:281–301. [PubMed: 10741850]
46. Duan J, Duan J, Zhang Z, Tong T. Irreversible cellular senescence induced by prolonged exposure to H2O2 involves DNA-damage-and-repair genes and telomere shortening. Int J Biochem Cell Biol 2005;37:1407–1420. [PubMed: 15833273]
47. Parrinello S, Samper E, Krtolica A, Goldstein J, Melov S, Campisi J. Oxygen sensitivity severely limits the replicative lifespan of murine fibroblasts. Nat Cell Biol 2003;5:741–747. [PubMed: 12855956]
48. Passos JF, Von Zglinicki T. Oxygen free radicals in cell senescence: Are they signal transducers? . Free Radic Res 2006;40:1277–1283. [PubMed: 17090417]
49. Allen RG, Tresini M. Oxidative stress and gene regulation. Free Radic Biol Med 2000;28:463–499. [PubMed: 10699758]
50. Hall AG. Review: The role of glutathione in the regulation of apoptosis. Eur J Clin Invest 1999;29:238–245. [PubMed: 10202381]
51. Ueda S, Masutani H, Nakamura H, Tanaka T, Ueno M, Yodoi J. Redox control of cell death. Antioxid Redox Signal 2002;4:405–414. [PubMed: 12215208]
52. Estrela JM, Ortega A, Obrador E. Glutathione in cancer biology and therapy. Crit Rev Clin Lab Sci 2006;43:143–181. [PubMed: 16517421]
53. Kwon YW, Masutani H, Nakamura H, Ishii Y, Yodoi J. Redox regulation of cell growth and cell death. Biol chem 2003;384:991–996. [PubMed: 12956415]
54. Cristofalo VJ, Lorenzini A, Allen RG, Torres C, Tresini M. Replicative senescence: a critical review. Mech Ageing Dev 2004;125:827–848. [PubMed: 15541776]
55. Rebrin I, Sohal RS. Pro-oxidant shift in glutathione redox state during aging. Adv Drug Deliv Rev 2008;60:1545–1552. [PubMed: 18652861]
56. Keogh BP, Allen RG, Pignolo R, Horton J, Tresini M, Cristofalo VJ. Expression of hydrogen peroxide and glutathione metabolizing enzymes in human skin fibroblasts derived from donors of different ages. J Cell Physiol 1996;167:512–522. [PubMed: 8655605]
57. Balin AK, Fisher AJ, Anzelone M, Leong I, Allen RG. Effects of establishing cell cultures and cell culture conditions on the proliferative life span of human fibroblasts isolated from different tissues and donors of different ages. Exp Cell Res 2002;274:275–287. [PubMed: 11900488]
58. Rebrin I, Kamzalov S, Sohal RS. Effects of age and caloric restriction on glutathione redox state in mice. Free Radic Biol Med 2003;35:626–635. [PubMed: 12957655]

59. Sohal RS, Toy PL, Allen RG. Relationship between life expectancy, endogenous antioxidants and products of oxygen free radical reactions in the housefly, Musca domestica. Mech Ageing Dev 1986;36:71–77. [PubMed: 3762235]
60. Rebrin I, Bayne AC, Mockett RJ, Orr WC, Sohal RS. Free aminothiols, glutathione redox state and protein mixed disulphides in aging Drosophila melanogaster. Biochem J 2004;382:131–136. [PubMed: 15142037]
61. Toroser D, Sohal RS. Kinetic characteristics of native gamma-glutamylcysteine ligase in the aging housefly, Musca domestica L. Biochem Biophys Res Commun 2005;326:586–593. [PubMed: 15596139]
62. Toroser D, Sohal RS. Age-associated perturbations in glutathione synthesis in mouse liver. Biochem J 2007;405:583–589. [PubMed: 17461778]
63. Honda S, Matsuo M. Relationships between the cellular glutathione level and in vitro life span of human diploid fibroblasts. Exp Gerontol 1988;23:81–86. [PubMed: 3402554]
64. Orr WC, Radyuk SN, Prabhudesai L, Toroser D, Benes JJ, Luchak JM, Mockett RJ, Rebrin I, Hubbard JG, Sohal RS. Overexpression of glutamate-cysteine ligase extends life span in Drosophila melanogaster. J Biol Chem 2005;280:37331–37338. [PubMed: 16148000]
65. Shi ZZ, Osei-Frimpong J, Kala G, Kala SV, Barrios RJ, Habib GM, Lukin DJ, Danney CM, Matzuk MM, Lieberman MW. Glutathione synthesis is essential for mouse development but not for cell growth in culture. Proc Natl Acad Sci U S A 2000;97:5101–5106. [PubMed: 10805773]
66. Valverde M, Rojas E, Kala SV, Kala G, Lieberman MW. Survival and cell death in cells constitutively unable to synthesize glutathione. Mutat Res 2006;594:172–180. [PubMed: 16239016]
67. Soti C, Sreedhar AS, Csermely P. Apoptosis, necrosis and cellular senescence: chaperone occupancy as a potential switch. Aging Cell 2003;2:39–45. [PubMed: 12882333]
68. Harris SL, Levine AJ. The p53 pathway: positive and negative feedback loops. Oncogene 2005;24:2899–2908. [PubMed: 15838523]
69. Hussain SP, Harris CC. p53 biological network: at the crossroads of the cellular-stress response pathway and molecular carcinogenesis. J Nippon Med Sch 2006;73:54–64. [PubMed: 16641528]
70. Brooks CL, Gu W. Ubiquitination, phosphorylation and acetylation: the molecular basis for p53 regulation. Curr Opin Cell Biol 2003;15:164–171. [PubMed: 12648672]

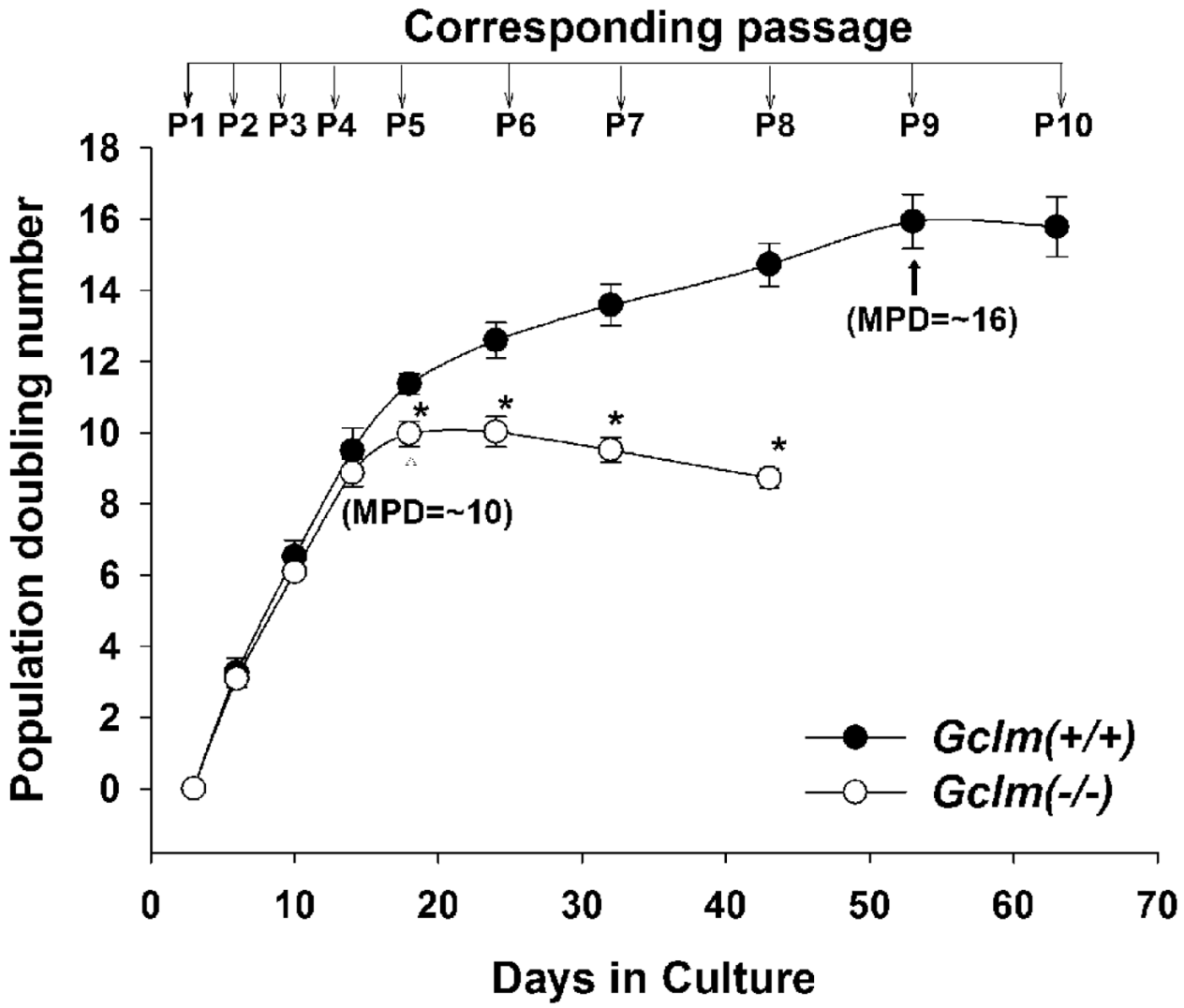

Fig. 1.

Decreased proliferative span and growth rate in *Gclm*(−/−) MFFs. The proliferative capacity is expressed as population-doubling (PD) numbers, derived from the equation as described in "Materials and Methods". *Gclm*(−/−) cells revealed growth retardation starting at P5 and a smaller maximal PD (MPD). Data are reported as means ± S.E. for six to eight individual wells of MFF cultures for each group, and three independent experiments. **p* <0.05, comparing *Gclm* (+/+) and *Gclm*(−/−) cells at the same passage number.

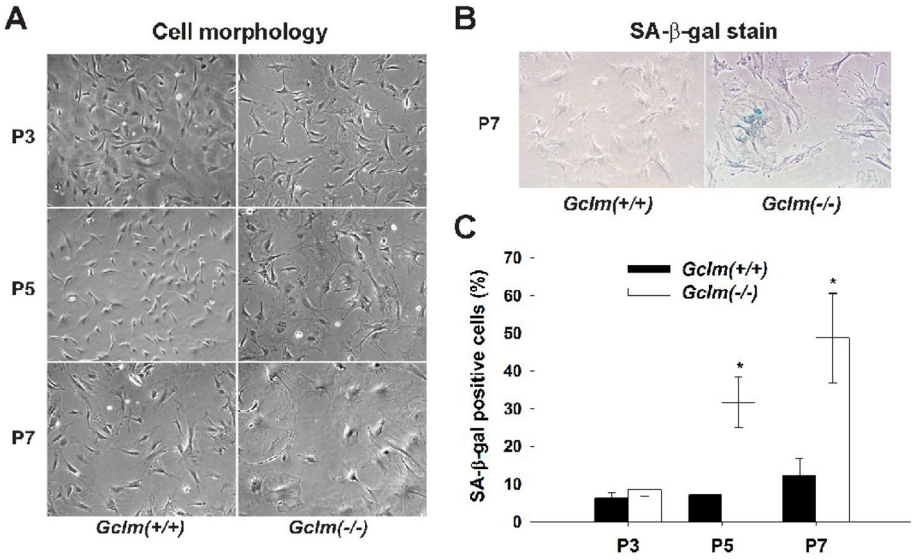

Fig. 2.

Premature senescence morphology and increased SA-β-gal activity in *Gclm*(−/−) MFFs. (***A***) General morphology of the MFF cells. Starting at passage 5 (**P5**), *Gclm*(−/−) cells became enlarged and flattened, with a decreased nucleus-to-cytoplasm ratio. (400x) (***B***) Representative images of SA-β-gal staining in *Gclm*(+/+) and *Gclm*(−/−) cells at P7. (400x) (***C***) Quantification of the SA-β-gal-staining. The number of positive (*blue stained*) cells was counted in 200 cells and SA-β-gal activity was expressed as percent of positive cells in total cells. *: $p < 0.05$, comparing *Gclm*(+/+) and *Gclm*(−/−) cells at the same passage number.

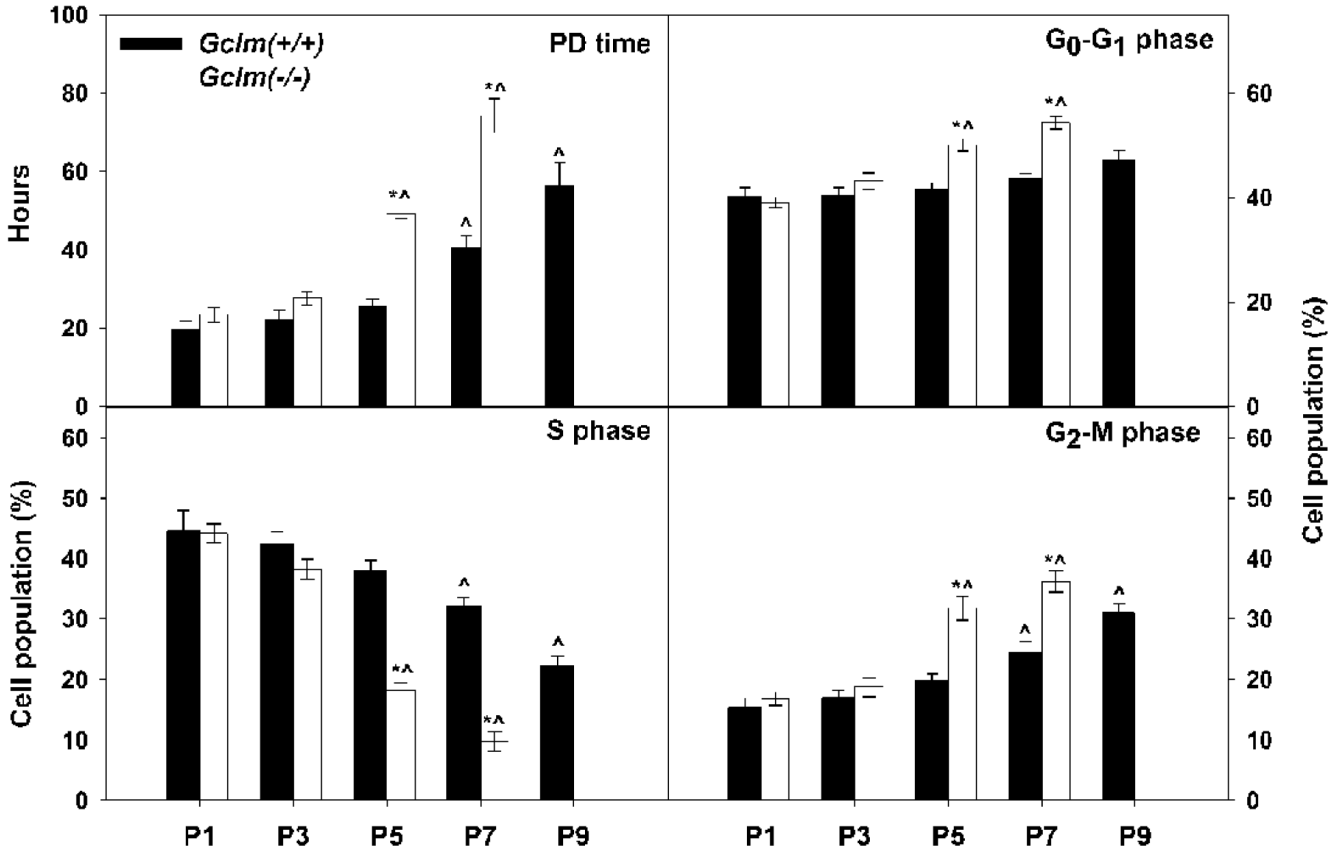

Fig. 3.

Growth arrest at the G**1**/S and G**2**/M boundaries in senescent *Gclm*(−/−) MFFs. *Upper left*: Population-doubling (PD) time (in hours) was determined from the growth rate assay as described in "Materials and Methods". *Lower left and at right*: Cell population (%) in each cell-cycle phase was determined by flow-cytometry. Data are reported as means ± S.E. of three or four individual wells of cell cultures for each group. *p <0.05, comparing *Gclm*(+/+) and *Gclm*(−/−) cells at the same passage number. ^p <0.05, compared with P1 cells of the same genotype.

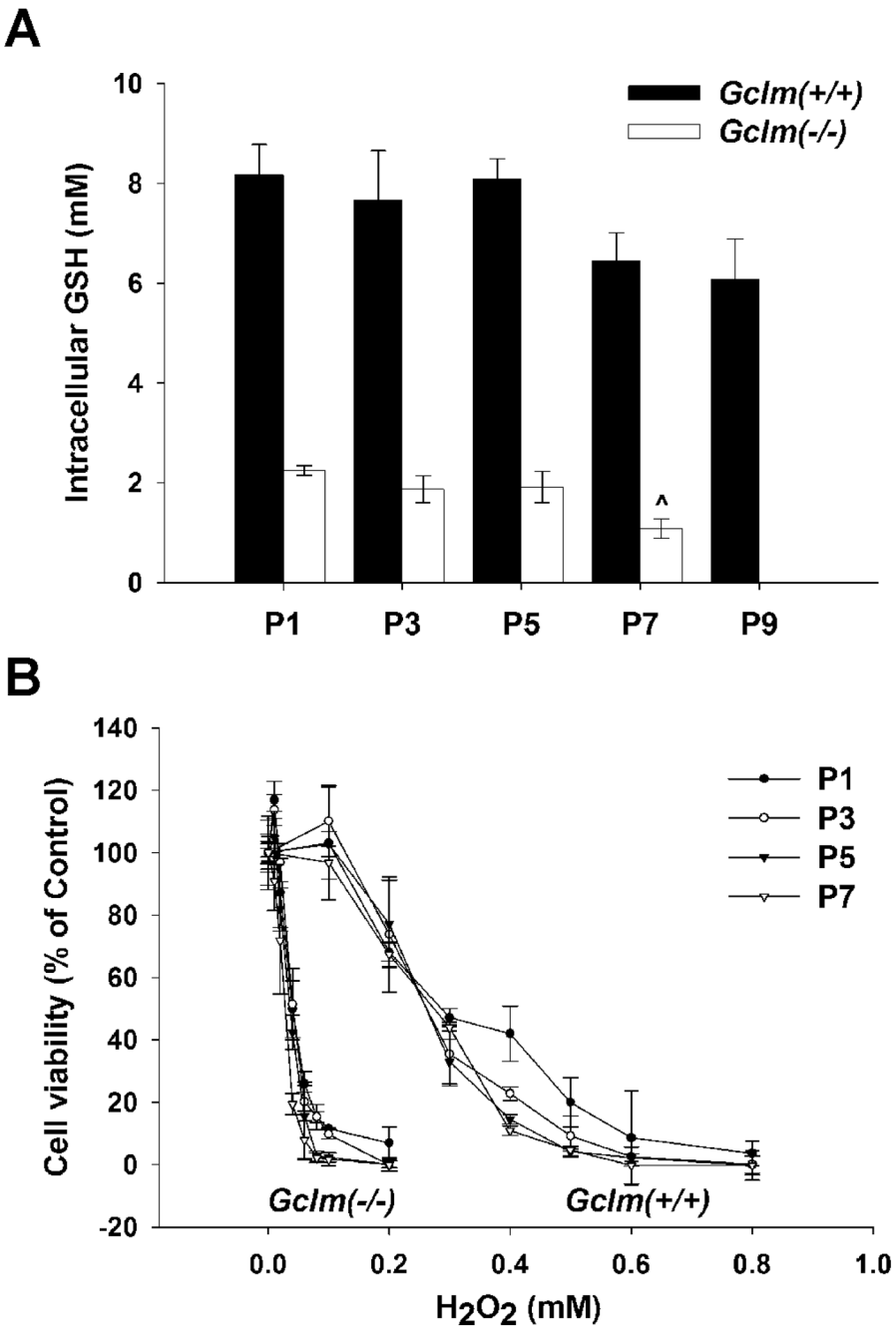

Fig. 4.

Intracellular GSH levels and response to H_2O_2 in *Gclm*(+/+) versus *Gclm*(−/−) MFFs. (***A***) Intracellular GSH levels at P1 through P9 were determined spectrophotofluorometrically using *o*-phthalaldehyde. (***B***) Cell viability, subsequent to H2O2 treatment for 8 h, was determined by the MTT assay and expressed as percent of untreated cells (100% viable). Data are reported as means ± S.E. for three or four individual wells of MFF cultures for each group.

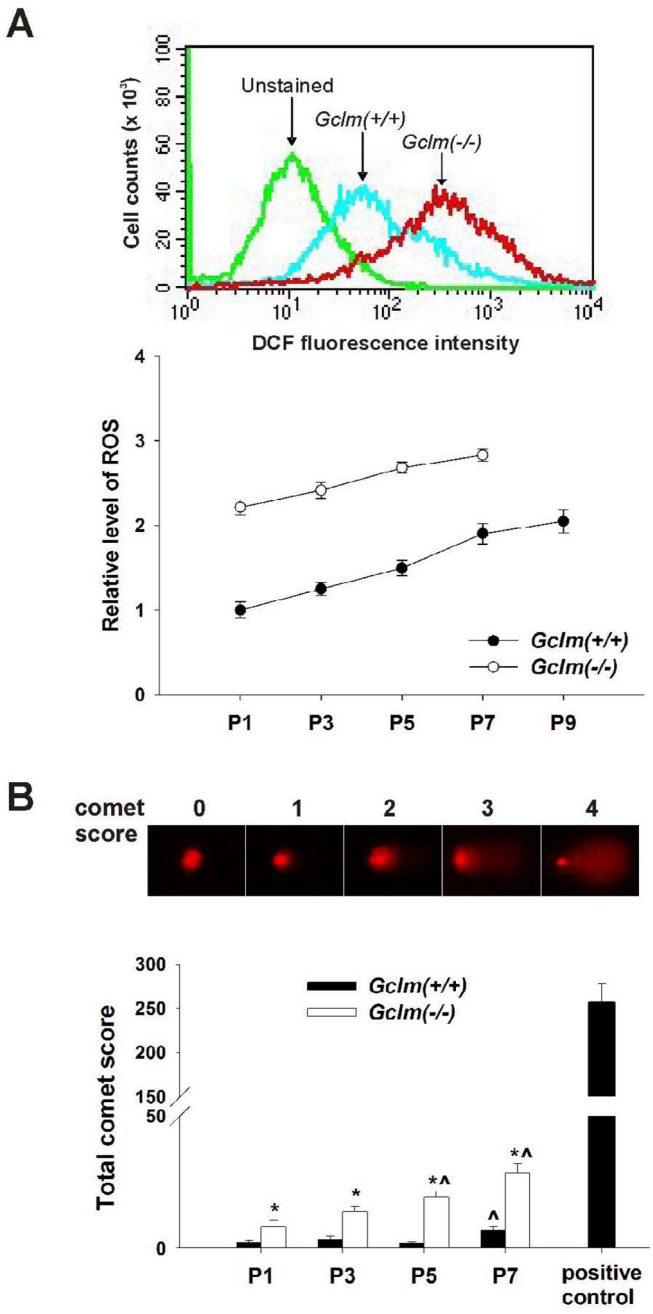

Fig. 5.

ROS formation and DNA damage in *Gclm*(+/+) versus *Gclm*(−/−) MFFs. (***A***) Intracellular ROS levels were determined using H_2O_2-activated CM-H2DCFDA as the fluorescent probe by flow cytometry. Cells in the absence of probe (unstained) were used to generate negative baseline. Fluorescent intensity in P1 *Gclm*(+/+) wild-type cells was set as the control; ratio to this control level is expressed as the relative ROS level. (***B***) DNA strand breaks were determined by the alkaline comet assay. Comet was scored from 0 to 4, based on the length of the comet tail. The extent of DNA damage was expressed as the total comet score in 150–200 cells, as described in "Materials and Methods". P1 *Gclm*(+/+) cells, treated with 100 μM H_2O_2 for 2 h, was used as the positive control. Data are reported as means ± S.E. of three or four individual wells of

MFF cultures for each group. *p <0.05, comparing *Gclm*(+/+) and *Gclm*(−/−) cells at the same passage number, ^p <0.05, compared with P1 cells of the same genotype.

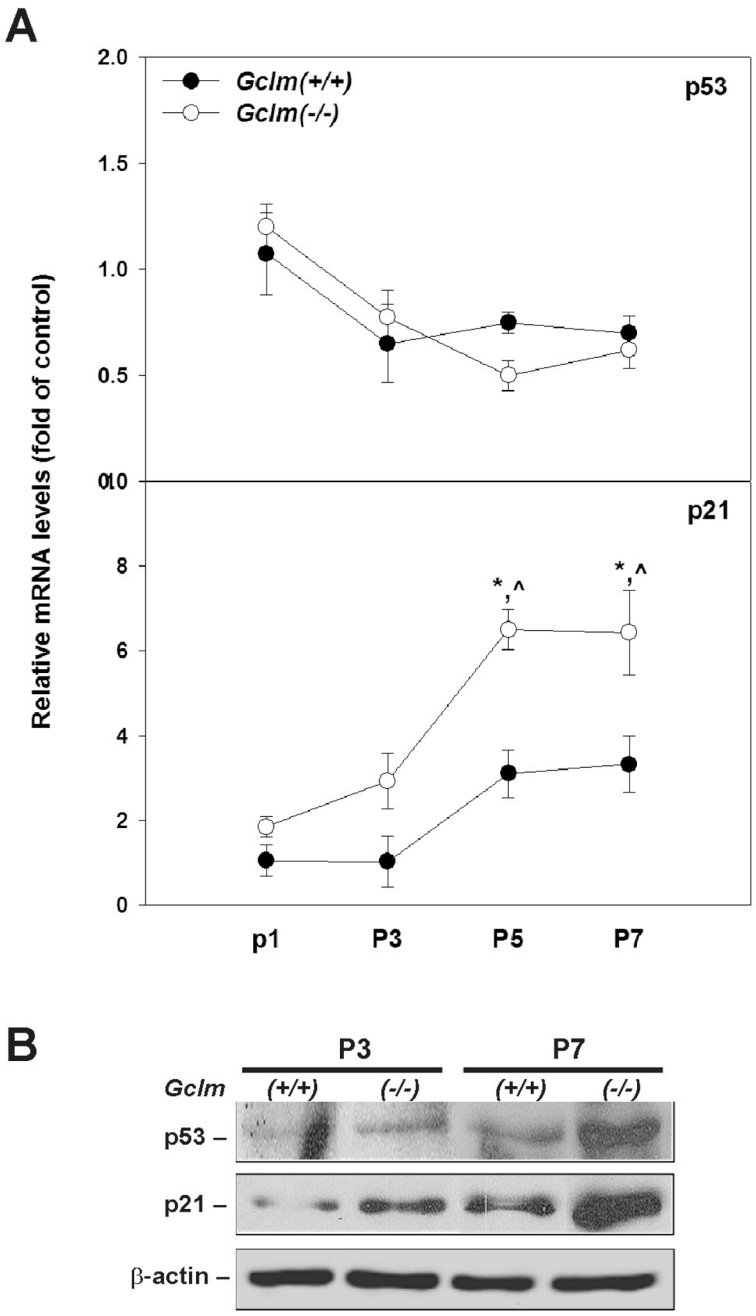

Fig. 6.

Induction of p53 and p21 in senescent *Gclm*(−/−) MFFs. (***A***) The mRNA levels of p53 and p21 were quantified by Q-PCR. The mRNA level for each gene in P1 *Gclm*(+/+) cells was set as the control (= 1.0). Relative mRNA levels are expressed as fold of the control after normalization with β-Actin. Data are reported as means ± S.E. of 3–4 individual cell cultures for each group. **p* <0.05, comparing *Gclm*(+/+) and *Gclm*(−/−) cells at the same passage number; ^*p* <0.05, compared with P1 cells of the same genotype. (***B***) Semi-quantification of p53 and p21 proteins in *Gclm*(+/+) versus *Gclm*(−/−) cells. Western immunoblot analysis was carried out on p53, p21 and β-actin in nuclear extracts (30 μg) from cells. Inductions of p53 and p21 were observed in senescent *Gclm*(−/−) cells (P7).

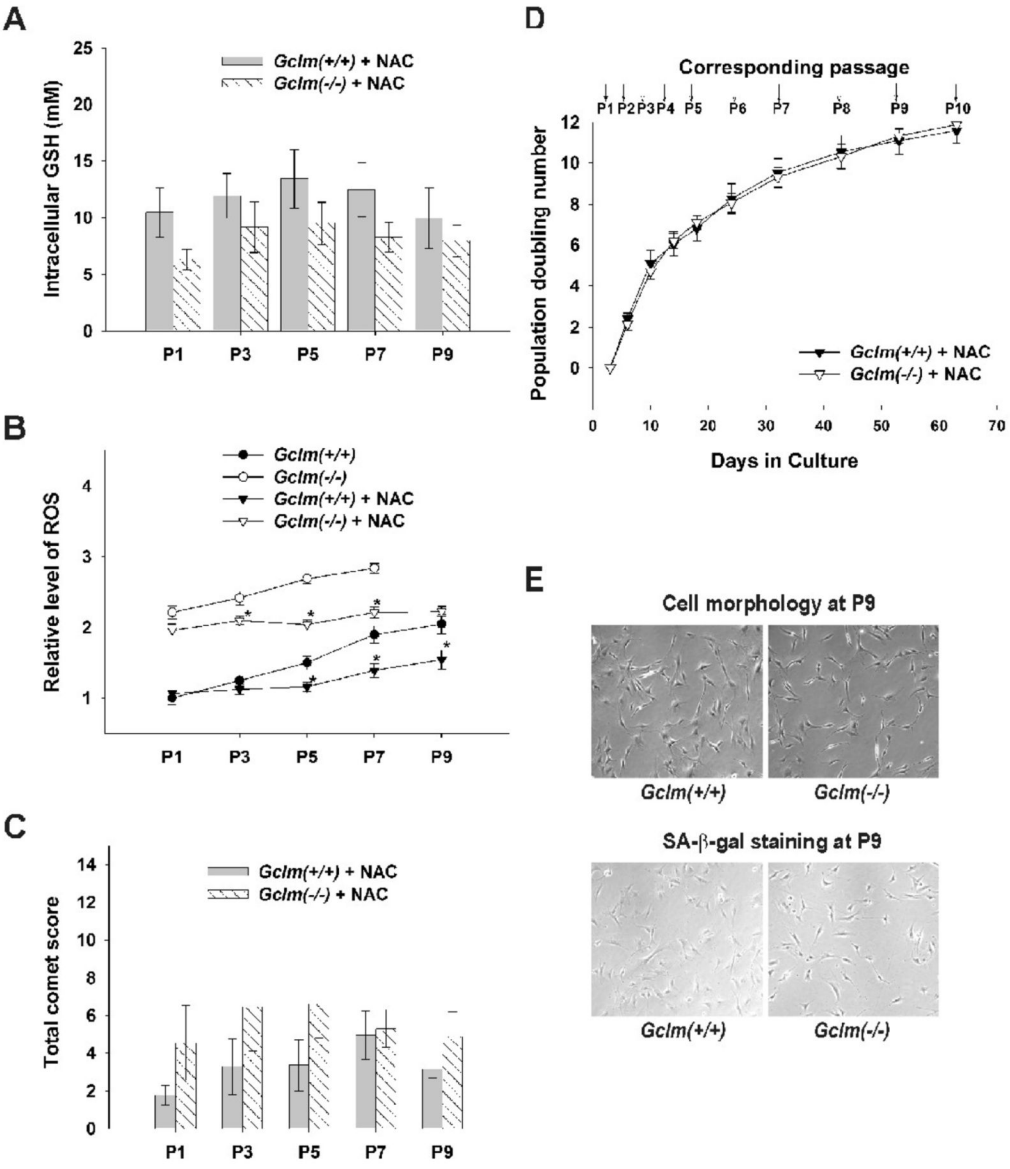

Fig. 7.

Prevention of premature senescence in *Gclm*(−/−) MFFs by NAC supplementation. Freshly made NAC (final concentration 5 mM) was added to the standard culture medium starting at P1. (***A***) Intracellular GSH levels in NAC-treated *Gclm*(−/−) cells approach those seen in *Gclm* (+/+) cells. (***B***) Intracellular ROS levels were lowered by NAC treatment in *Gclm*(−/−) cells, but remained higher than those in *Gclm*(+/+) cells—with or without NAC treatment. (***C)*** DNA strand breaks remained at control levels in NAC-treated *Gclm*(−/−) cells, compared with NAC-treated *Gclm*(+/+) cells. (***D***) Similar growth profiles were observed in NAC-treated *Gclm*(+/+) and NAC-treated *Gclm*(−/−) cells. (***E***) Pre-senescent cell morphology and negligible SA-β-gal-positive staining are the same in P9 NAC-treated cells of both genotypes. Data are reported as means ± S.E. of three or four individual wells of MFF cultures for each group. **p* <0.05, comparing untreated and NAC-treated MFFs of the same genotype at the same passage number.